

Supporting Information

Selective and efficient removal of perrhenate by an imidazolium based hexapodal receptor in water medium

Rajib Ghosh, Tamal Kanti Ghosh, and Pradyut Ghosh*

School of Chemical Sciences, Indian Association for the Cultivation of Science 2A & 2B Raja S. C. Mullick Road, Kolkata – 700032. E-mail: icpg@iacs.res.in

Table of Contents

1. Material	Page 3S
2. Spectroscopic instrumentation	Page 3S
3. X-ray crystallography	Page 3S
4. Synthesis and characterization	Page 4S
5. Experimental section	Page 5S-6S
6. Crystallographic Details	Page 6S
7. ^1H , ^{13}C NMR & ^{13}C -DEPT -135, FT-IR spectra of [L.6Br]	Page 7S-8S
8. ESI-MS spectrum of [L.6Br] and ^1H NMR in D_2O	Page 9S-10S
9. ^1H NMR titration profile of [L.6Br] with various anions.	Page 11S
10. ^1H NMR titration profile of [L.6Br] with different equivalent of NaReO_4	Page 12S
11. ^1H NMR titration profile of [L.6Br] with different equivalent of NaClO_4	Page 12S
12. Plot and table of thermodynamic parameter obtained from ITC	Page 13S-15S
13. Optical photograph of crystal (Complex [L.6ReO ₄])	Page 16S
14. Thermal ellipsoid plot of single crystal X-ray structure of Complex-[L.6ReO ₄]	Page 16S
15. Pictorial representation of the various conformer of hexapodal receptor	Page 17S
16. Crystal packing diagram of Complex 1	Page 17S
17. ^1H , ^{13}C NMR & ^{13}C -DEPT -135 spectra of Complex [L.6ReO ₄]	Page 18S-19S
18. ESI-MS spectrum of Complex [L.6ReO ₄]	Page 20S
19. PXRD of [L.6Br] and Complex [L.6ReO ₄]	Page 20S
20. Stack plot enlarge PXRD pattern of Complex [L.6ReO ₄] and its comparison with simulated pattern.	Page 21S
21. Stack plot of ^1H -NMR spectra of pure crystal and complex [L.6ReO ₄]	Page 22S
22. Thermal ellipsoid plot of single crystal X-ray structure of recrystallized precipitate Complex [L.6ReO ₄] with all hydrogen bond distance.	Page 22S
23. Table of ReO_4^- removal efficiency of [L.6Br] in presence of different anion	Page 23S
24. FT-IR spectrum of Complex 1 from mixed anion	Page 24S
25. Table of ReO_4^- removal efficiency of [L.6Br] in different pH value of solution	Page 24S
26. ^1H -NMR spectrum of [L.6Br] in H_2O at different pH range	Page 25S
27. ^1H -NMR spectrum of Complex [L.6ReO ₄] in $\text{DMSO}-d_6$, after being immersed the Complex [L.6ReO ₄] in different pH water solution for 12 hours	Page 25S
28. ^1H & ^{13}C NMR spectra of recycled [L.6Br]	Page 26S
29. Stack ^1H & ^{13}C NMR spectra of L and recycled Complex [L.6ReO ₄]	Page 27S
30. PXRD stack plot of Recycle receptor [L.6Br]	Page 28S
31. IR Spectra recycle receptor [L.6Br]	Page 28S
32. ReO_4^- removal efficiency of recycle [L.6Br]	Page 29S
33. References	Page 29S

1. Materials: Hexakis(bromomethyl)-benzene,1-ethyl- imidazole, NaReO_4 were purchased from Sigma-Aldrich and were used as received. NaOH , HNO_3 , Na_2SO_4 , NaNO_3 , NaCl , TBAH_2PO_4 , NaClO_4 , NaBF_4 and other reagent were analytically pure and used as received. ReO_4^- stock solution was prepared by dissolving desired amount of NaReO_4 solid in Mili-Q ultrapure water.

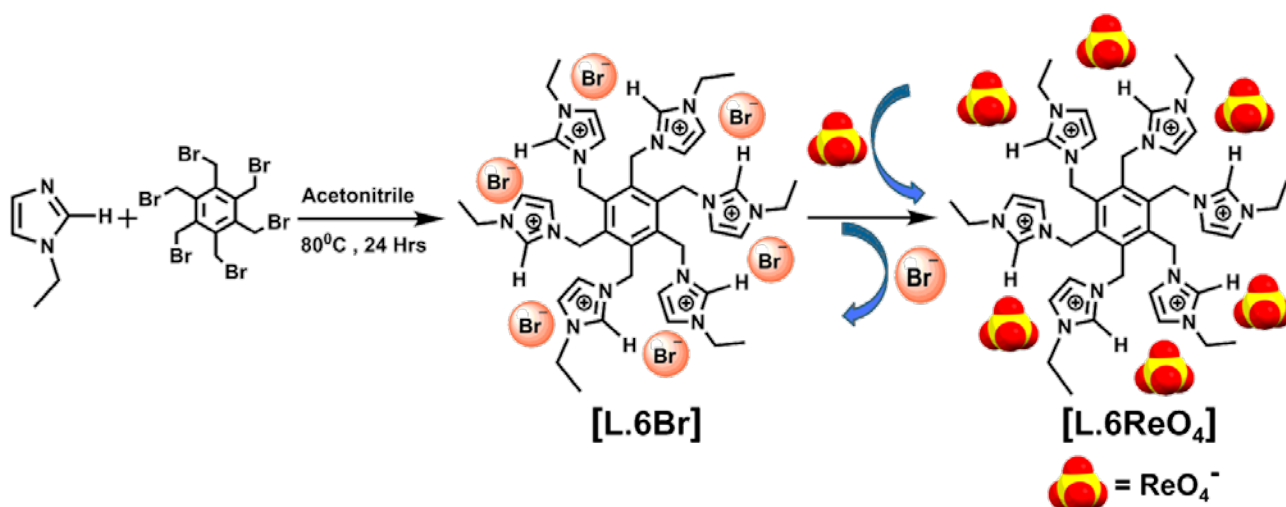
1.1 Spectroscopic Measurement Instrumentation:

NMR experiments were carried out on FT-NMR Bruker DPX 300 MHz NMR spectrometer. All the samples for NMR spectroscopy were prepared by dissolving the samples in $\text{DMSO-}d_6$ and H_2O (Locking was performed using a capillary tube filled with D_2O) having concentrations $\approx 10^{-3}$ (M). Chemical shifts for ^1H and ^{13}C NMR were reported in parts per million (ppm), calibrated to the residual solvent peak set. High resolution ESI-MS experiments were carried out with a Waters QtoF Model YA 263 mass spectrometer in positive ESI mode. Sample for mass spectrometry was prepared by dissolving the compound in $\text{CH}_3\text{CN}/\text{H}_2\text{O}$ with concentration $\approx 10^{-6}$. The concentration of ReO_4^- in solution were measured by inductively coupled plasma –atomic emission spectrometry(ICP-AES ,Perkin Elmer optima 2100 DV).The FT-IR was recorded on a SHIMADZU FTIR-8400S infrared spectrophotometer with KBr pellets.

1.2 X-Ray single-Crystal structure measurement:

The crystallographic details of Complex [**L.6ReO₄**] are given in (Table S1). In each case, a crystal of suitable size was dipped in paratone oil after collecting from the mother liquor. Further, it was mounted on nylon loop and data collected at 120k under cold nitrogen gas stream. The X-ray diffraction data for the crystal collected on a Bruker D8 Venture Microfocous diffractometer equipped with a PHOTON II detector, using $\text{MoK}\alpha$ ($\lambda = 0.71073$ Å) radiation, controlled by the APEX3(v2017.3-0) software package and processes using SAINT^[1]. The raw data were integrated and corrected for Lorentz and polarization effects using the Bruker APEX II/APEX III program suite. Integration and reduction were processed with SAINT^[1] software. An empirical absorption correction was applied to the collected reflections with SADABS.^[2] The structures were solved by direct methods using SHELXTL^[3] and were refined on F^2 by the full-matrix least-squares technique using the SHELXL-2014^[4] program package. Graphics were generated using PLATON-97^[5] and MERCURY 3.7.^[6] Crystallographic data have been deposited with the CCDC (1948657-1956499).

2 Synthesis and characterization



Scheme S1. Synthesis route of receptor [L.6Br] and its anion exchange application

3. Synthesis and characterization of Receptor [L.6Br]:

Hexakis(bromomethyl)-benzene 0.318 g (0.5 mmol) was dissolved in 40 ml of acetonitrile at 80 °C under argon atmosphere. Then 1-ethyl- imidazole 0.315ml (3.25 mmol) was added in drop by drop fashion to the refluxing solution over a long period of time (6 hours). After the addition was completed, the solution was allowed to reflux till 48 hours and during this time we observed precipitation of yellowish white solid of [L.6Br]. After completion, the solution was filtered and solid mass was washed with dry acetonitrile solution for removal of excess 1-ethyl- imidazole. Then solid mass was dried. Then solid mass was dissolved in minimum amount of mild hot water. Finally the water medium was dried in open air in a flat surface for 48 hours. Then solid mass was dried in an oven at 60 °C for 48 hours to remove a little trace of water from it (Yield 75%).

¹H NMR (DMSO-*d*₆, 298K, 300 MHz) δ ppm: 1.43-1.38 (t, 18H, -CH₃), 4.22-4.18 (q, 12H, -CH₂), 5.76 (s, 12H), 7.80 (bs, 6H), 7.76 (bs, 6H), 9.41 (bs, 6H). ¹³C NMR (DMSO-*d*₆, 298K, 75 MHz) δ ppm: 15.08, 44.21, 47.35, 121.42, 122.67, 136.12, 138.29. ¹³C- DEPT-135 NMR: 15.55 (CH₃), 44.77 (CH₂), 47.83 (CH₂), 121.93 (CH), 123.05 (CH), 136.53 (CH). ESI-MS: m/z: calcd for C₄₂H₆₀Br₅N₁₂ [L.5Br]⁺ 1131.0934, found 1131.0924; calcd for C₄₂H₆₀Br₄N₁₂ [L.4Br]²⁺, 526.0873, found 526.0863.

3.1 Synthesis of complex [L.6ReO₄]:

An aliquot of 1ml 12.3 Mm aqueous solution of [L.6Br] was added to the 10 equivalent aqueous NaReO₄ solutions. Then the mixture was stirred for 5 min with 200 rpm and a white solid precipitate was observed. Then the white solid mass was separated by whatman grade 1 filter paper. Finally solid mass was dried in an oven at 60 °C for 48 hours and we get the complex [L.6ReO₄].

3.2 Characterization of extracted complex [L.6ReO₄]:

¹H NMR (DMSO-*d*₆, 298K, 300 MHz) δ ppm: 1.44-1.39 (t, 18H), 4.20-4.13 (q, 12H), 5.64 (s, 12H), 7.83(bs, 6H), 7.32 (bs, 6H), 8.84 (s, 6H). ¹³C NMR (DMSO-*d*₆, 298K, 75 MHz) δ ppm: 15.04, 44.58, 46.92, 121.97, 122.06, 135.69, 138.15. ¹³C- DEPT-135 NMR: 15.52 (CH₃), 45.06 (CH₂), 47.44 (CH₂), 122.52 (CH), 136.18 (CH). ESI-MS: m/z: calcd for C₄₂H₆₀N₁₂O₂₀Re₅ [L.5ReO₄]⁺ 1983.1773, found 1983.1762; calcd for C₄₂H₆₀N₁₂O₁₆Re₄ [L.4ReO₄]²⁺, 867.1221, found 867.1214.

4. Experimental Section:

4.1 Isothermal Titration Calorimetry:

The solution-state binding of [L.6Br] with ReO₄⁻ was analyzed by ITC experiments. In a typical ITC experiment, a solution of the anion as its tetrabutylammonium (TBA) salt in solvent was titrated into a solution of L at 298 K. The acetonitrile used for the studies were dried previously and for binary solvent mixture preparation, we used Mili-Q ultrapure water and added an adequate amount to the dry acetonitrile. Exothermic titration profiles were obtained for all titrations and subsequent fitting to a 'one set of site' binding model provided access to the association constant (K), enthalpy change (ΔH), entropy change (TΔS) and Gibb's free energy change (ΔG) of the binding processes. Blank titration data was subtracted from the titration data in order to obtain accurate thermodynamic parameters of binding. The titrations were performed in the triplicate manner and mean data are reported with standard deviations. Origin 7.0 was used for analysis. The upper panel of the VP-ITC output figure exhibits the heat pulses, which were observed experimentally in each titration step with respect to time. The lower panel presents the respective time integrals translating as the heat absorbed or evolved for each aliquot and its coherence to a one set of site binding model. During each titration, a solution of ligand ~ 1.2 mM was placed in the cell at 298 K temperature. This solution was then titrated with 28 injections of 10 μL each of a ~ 37.8 mM

guest solution. An initial delay of 240s was allowed before each titration. Interval of 220s was allowed between each injection and the stirring speed was set at 329 rpm.

4.2 Batch Experiment: All the extraction experiments were conducted at room temperature (25°C) using MiliQ water. The pH value of solution was adjusted by using NaOH and HNO₃ solution. For the all PXRD experiment 12.3Mm 1ml water solution of [**L.6Br**] was added to the 10 eqv ReO₄⁻ solution .In a typical extraction experiment the solution was stirred for 5 min with 200 rpm and separated by Whatman grade 1 filter paper to separate the solid mass for PXRD experiment.

4.3 pH effect study: The effect of pH for extraction of ReO₄⁻ was carried out by ranging pH values from 1 to 14. 4.1 mM 1ml of L was added to 10 ml of aqueous solution containing 600 ppm ReO₄⁻. After being stirred at a rate of 200 rpm for 5 minutes, and the resultant solution was centrifuged for 5 min and settled for 30 min. Finally, the solution was separated with a 0.45µm nylon membrane filter for ICP measurement.

4.4 Anion extraction selectivity experiment: The effect of interfering anion was studied by adding 10 equivalent different anion are Na₂SO₄(5.7mM), NaNO₃(6.1 mM), NaCl(5.4 mM), TBAH₂PO₄(5.8 mM), NaClO₄(5.7 mM), NaBF₄(5.3 mM), TBAAcO(6.0 mM) in a solution NaReO₄(6.9 mM) and [**L.6Br**] (0.76 mM). After being stirred at a rate of 200 rpm for 5 minutes, and the resultant solution was centrifuged for 5 min and settled for 30 min. Finally, the solution was separated with a 0.45µm nylon membrane filter for ICP measurement.

Table S1: Crystallographic details of the Complex [**L.6ReO₄**] and recrystallized Complex [**L.6ReO₄**] obtained from water-ACN solvent mixture.

Compound reference	Complex [L.6ReO₄]	Extracted complex [L.6ReO₄]
Chemical formula	C ₄₂ H ₆₀ N ₁₂ O ₂₆ Re ₆	C ₅₀ H ₇₂ N ₁₆ O ₂₄ Re ₆
Formula Mass	2266.22	2398.43
Crystal system	triclinic	triclinic
<i>a</i> /Å	9.8908(6)	9.616(4)
<i>b</i> /Å	10.5382(6)	12.479(5)
<i>c</i> /Å	15.9326(10)	15.960(7)
α /°	81.260(2)	109.630(8)
β /°	86.319(2)	102.850(8)
γ /°	68.024(2)	90.878(8)
Unit cell volume/Å ³	1522.08(16)	1750.3(13)
Temperature/K	120(2)	150(2)
Space group	<i>P</i> 1	<i>P</i> 1
No. of formula units per unit cell, <i>Z</i>	1	1
Radiation type	MoK α	MoK α
No. of reflections measured	14416	36844
No. of independent reflections	6336	7368
<i>R</i> _{int}	0.0631	0.1696
Final <i>R</i> _{<i>I</i>} values (<i>I</i> > 2 σ (<i>I</i>))	0.0646	0.0948
Final <i>wR</i> (<i>F</i> ²) values (<i>I</i> > 2 σ (<i>I</i>))	0.1780	0.2508
Final <i>R</i> _{<i>I</i>} values (all data)	0.0666	0.1383
Final <i>wR</i> (<i>F</i> ²) values (all data)	0.1811	0.2959
Goodness of fit on <i>F</i> ²	1.057	0.968
CCDC number	1948657	1956499

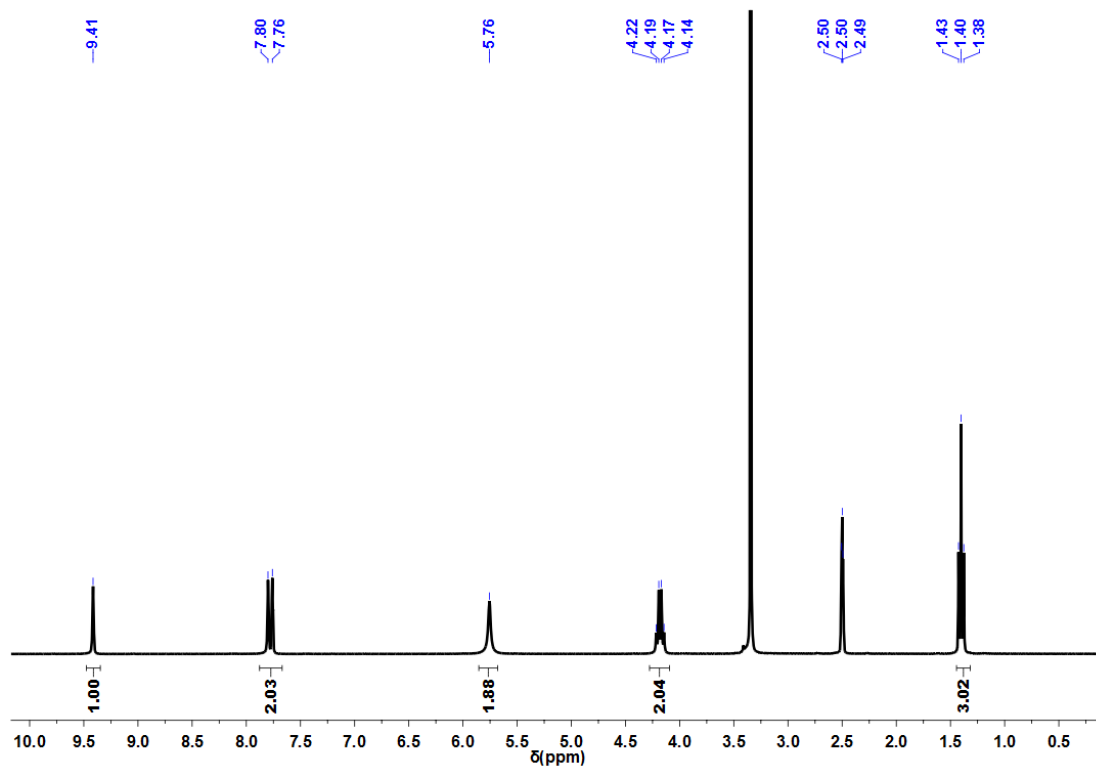


Fig. S1: ^1H -NMR spectrum of [L.6Br] in $\text{DMSO-}d_6$ at 298 K in 300 MHz

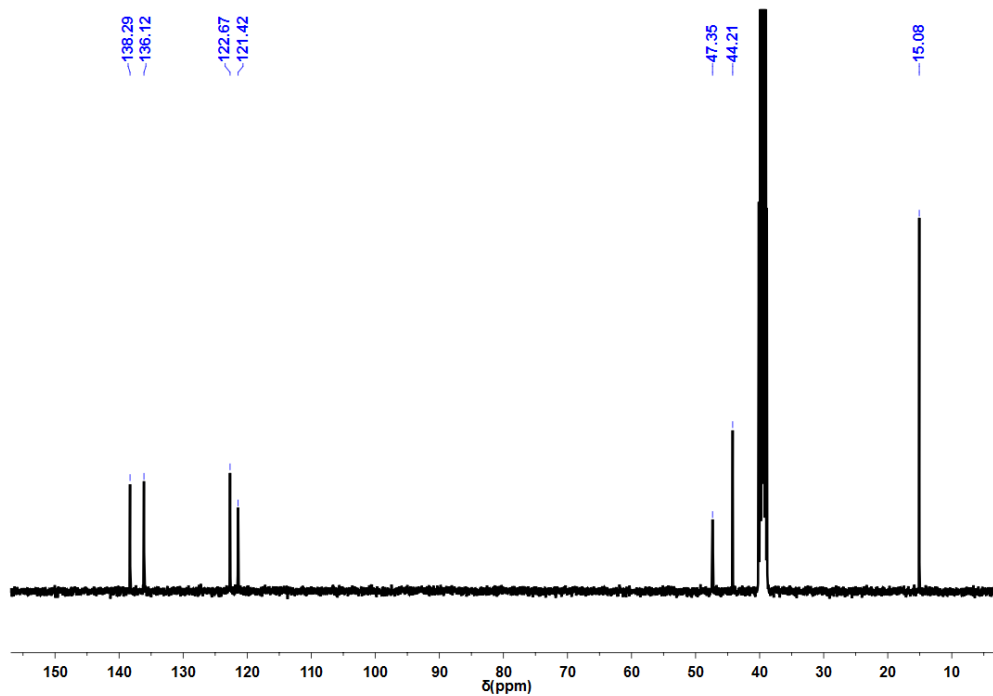


Fig. S2: ^{13}C -NMR spectrum of [L.6Br] in $\text{DMSO-}d_6$ at 298 K in 100 MHz

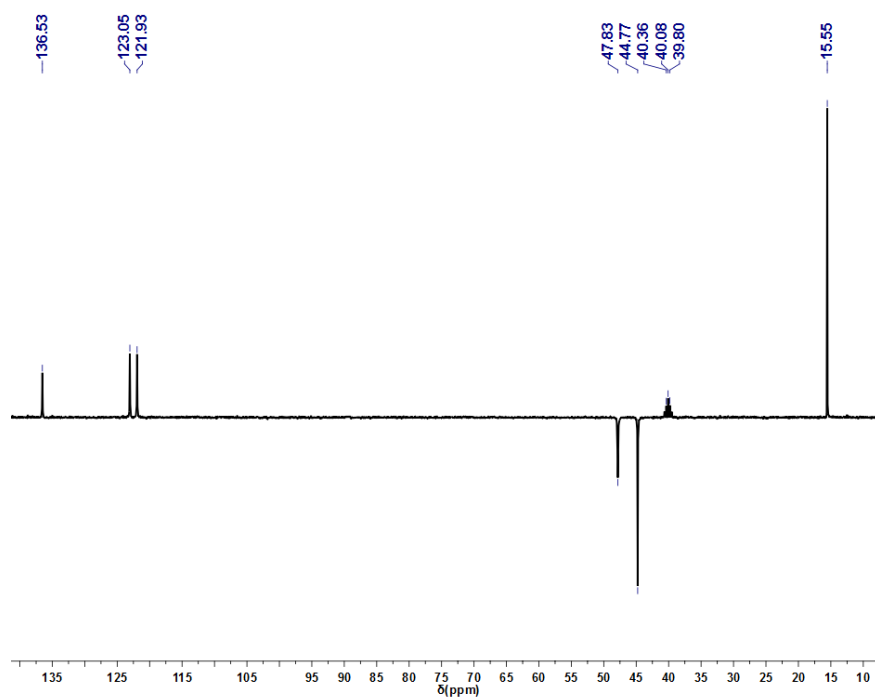


Fig. S3: ^{13}C -DEPT-135 spectrum of [L.6Br] in $\text{DMSO-}d_6$ at 298K in 75 MHz

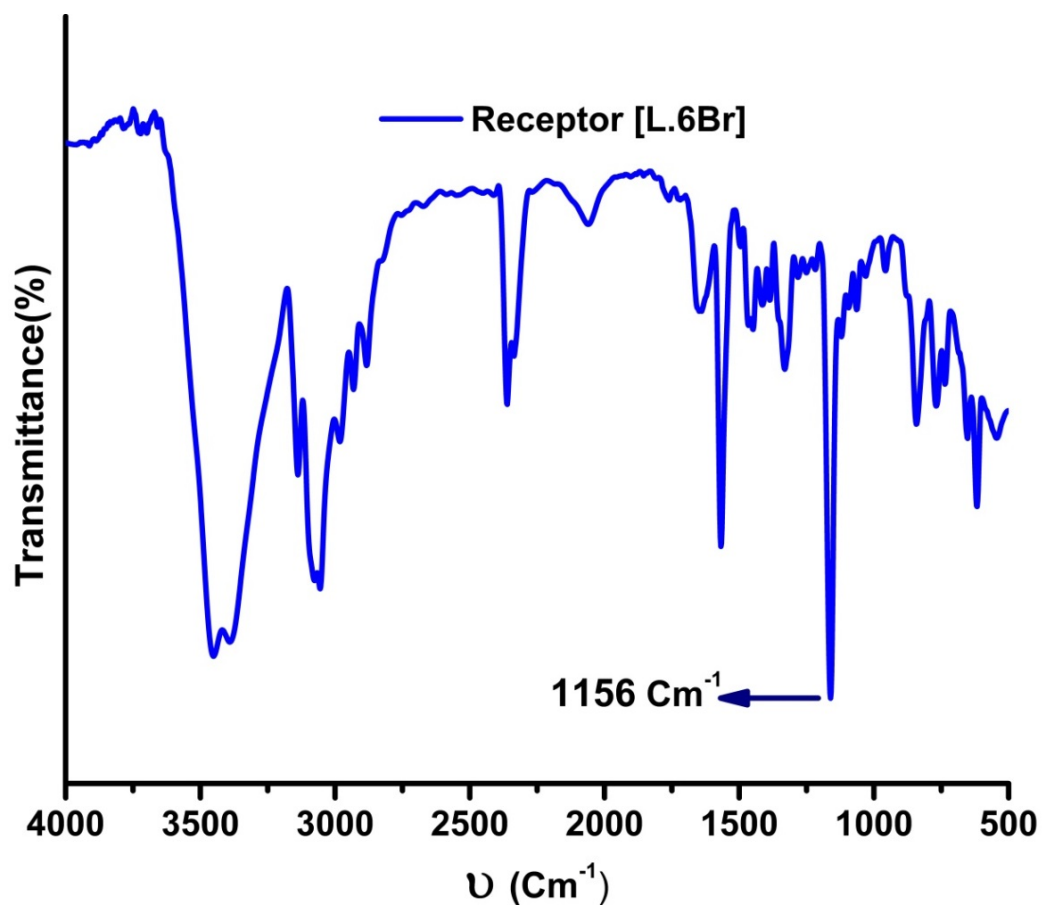


Fig. S4: FT-IR spectrum of receptor [L.6Br]

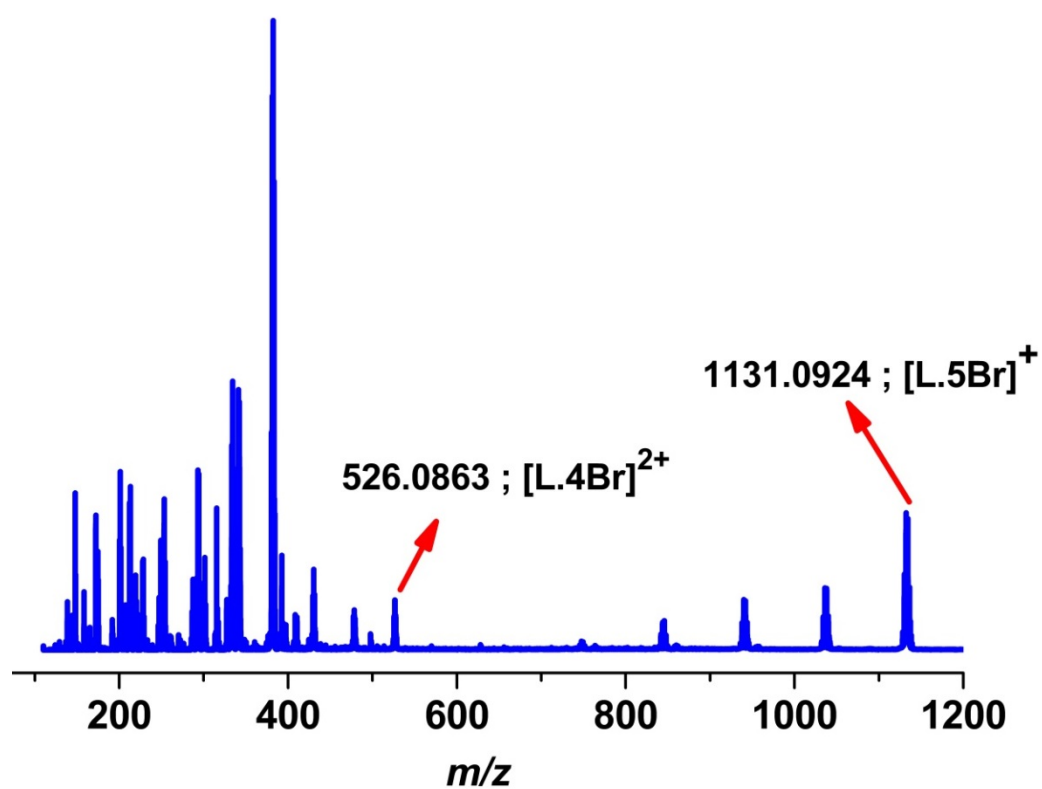


Fig. S5: ESI-MS (+ve) spectrum [L.6Br] at 298K.

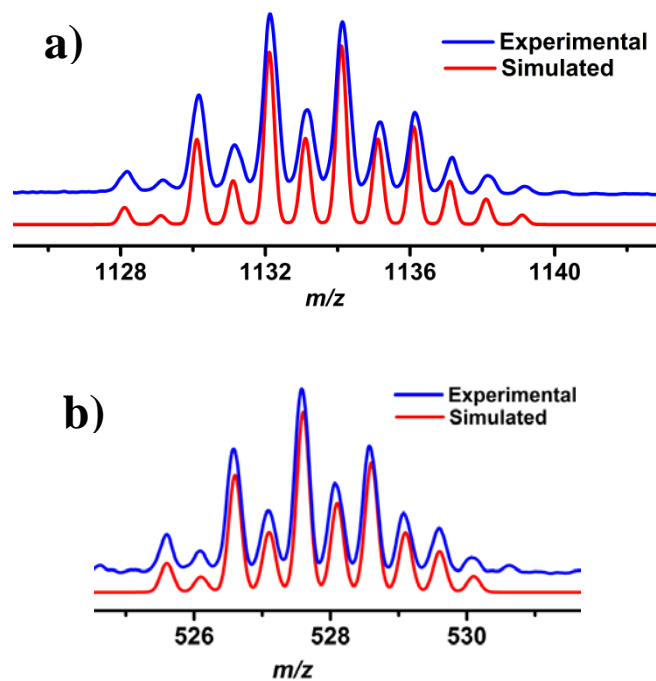


Fig. S6: Isotopic distribution of ESI-MS (+ve) spectrum of (a) $[L.5Br]^+$ and (b) $[L.4Br]^{2+}$ at 298K.

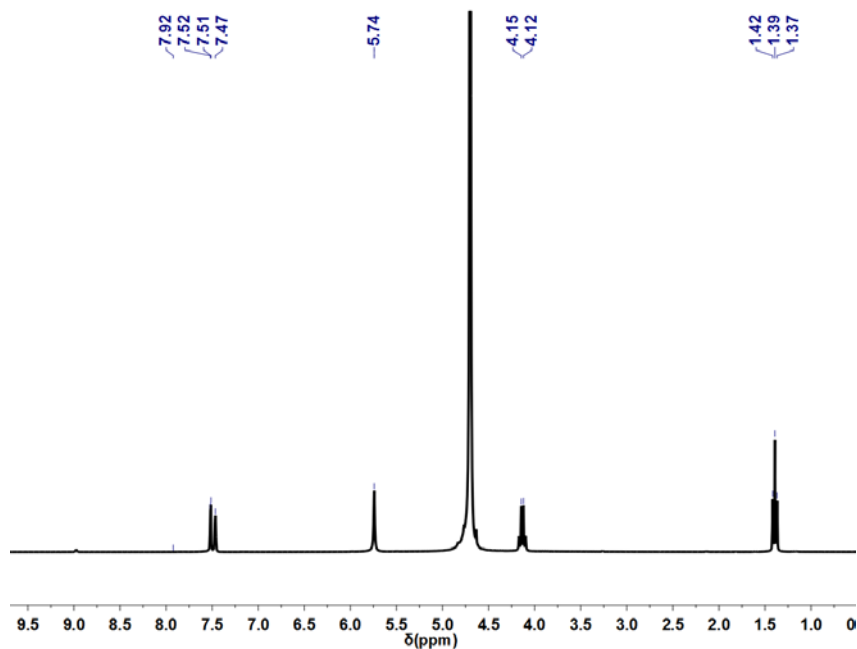


Fig. S7: $^1\text{H-NMR}$ spectrum of receptor **[L.6Br]** in D_2O at 298 K in 300 MHz

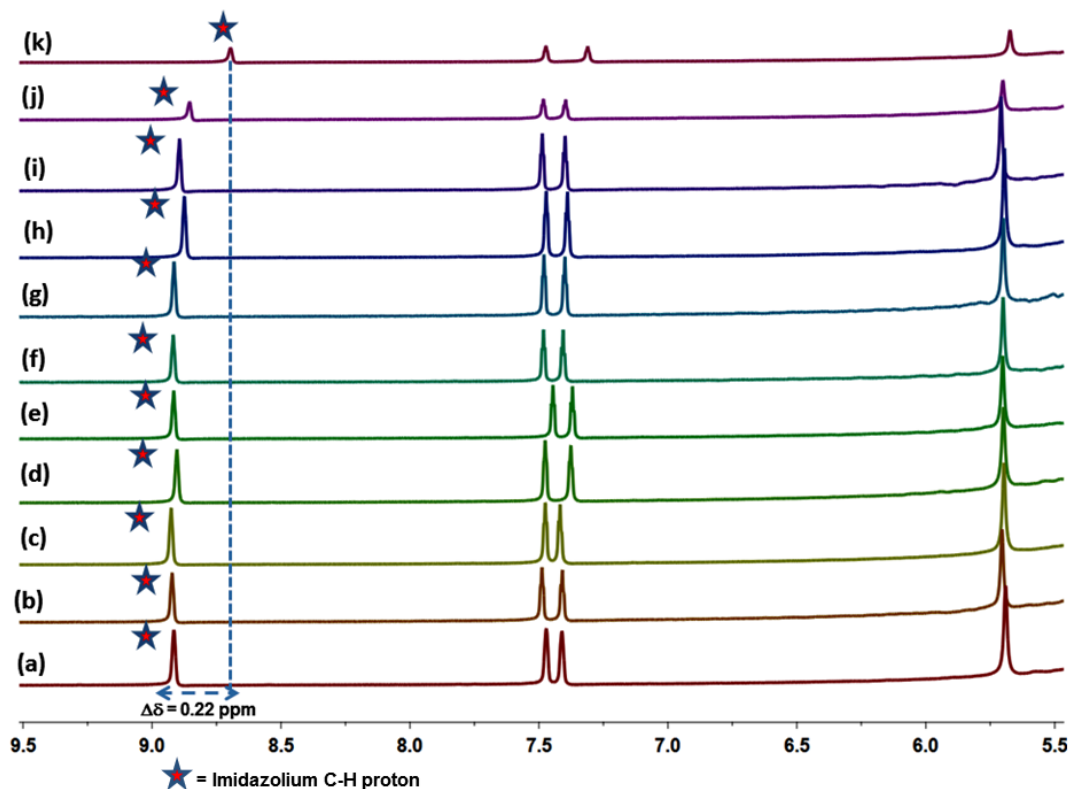


Fig. S8: Partial $^1\text{H-NMR}$ spectra of (a) Receptor **[L.6Br]** (9.3 mM) and **[L.6Br]** (9.3 mM) with 10 equivalents of (b) TBAF (c) TBACl (d) NaI (e) Na_2SO_4 (f) TBAH_2PO_4 (g) TBAAcO (h) NaNO_3 (i) TBABF_4 and (j) NaClO_4 (7 equivalent) (k) NaReO_4 (5 equivalent) in H_2O at 298 K (Locking was performed using a capillary tube filled with D_2O)

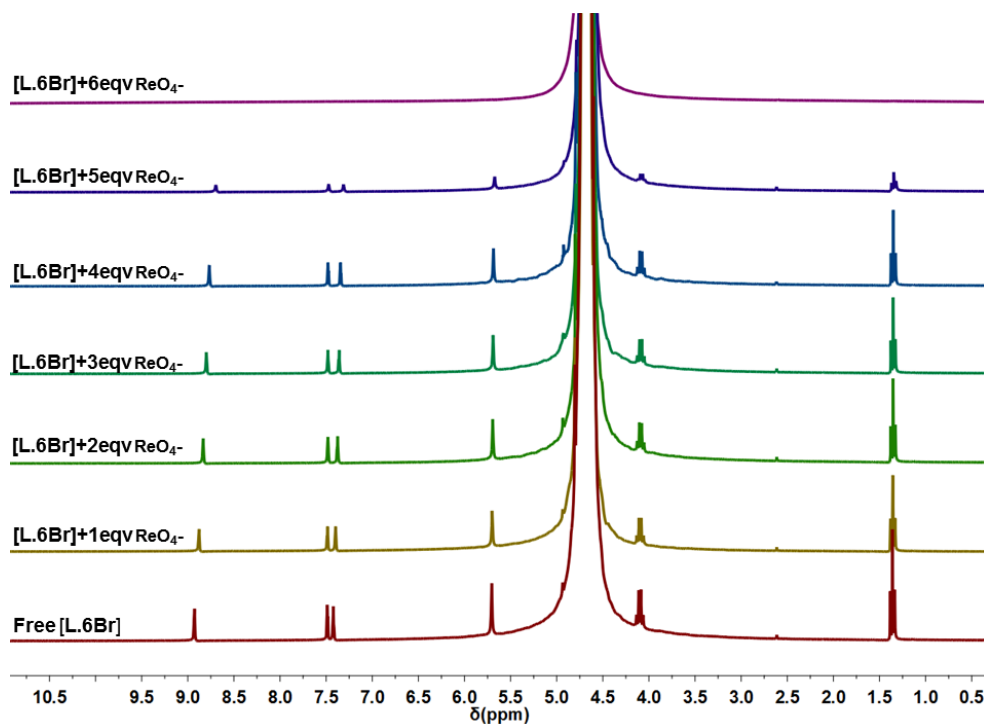


Fig. S9: $^1\text{H-NMR}$ spectrum of $[\text{L.6Br}]$ (14.4 mM) in H_2O with different equivalents of NaReO_4 in 300 MHz at 298 K. (Locking was performed using an capillary tube filled with D_2O)

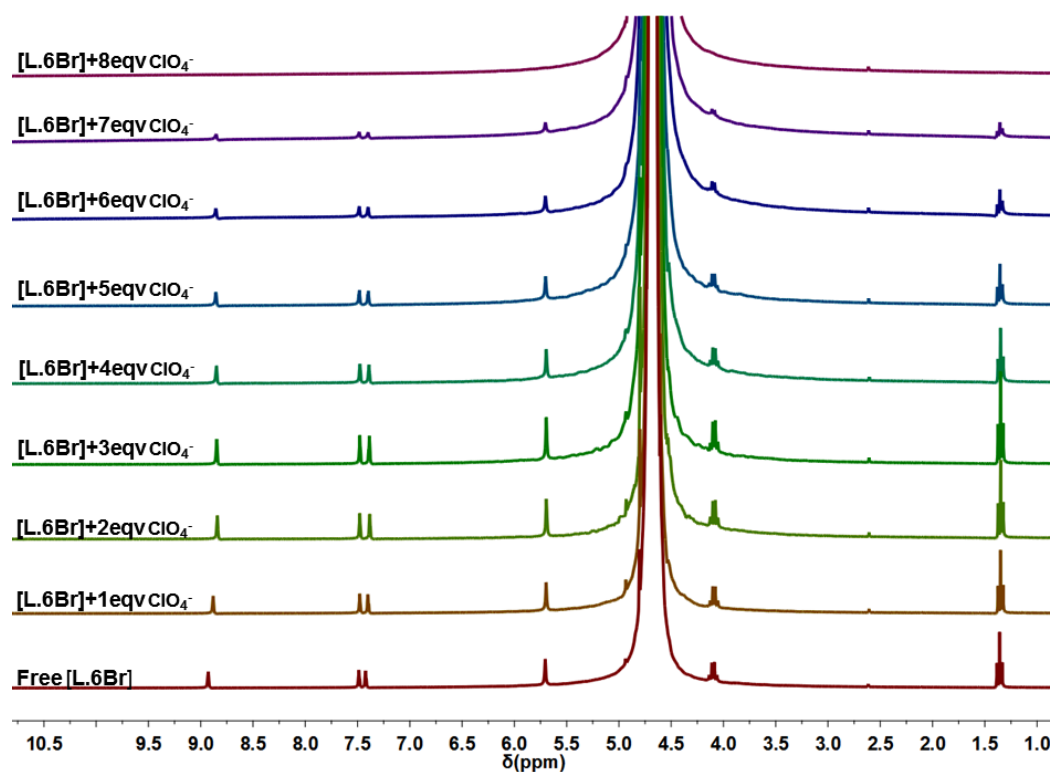


Fig. S10: $^1\text{H-NMR}$ spectrum of $[\text{L.6Br}]$ (14.8 mM) in H_2O with different equivalent of NaClO_4 in 300 MHz at 298 K. (Locking was performed using an capillary tube filled with D_2O)

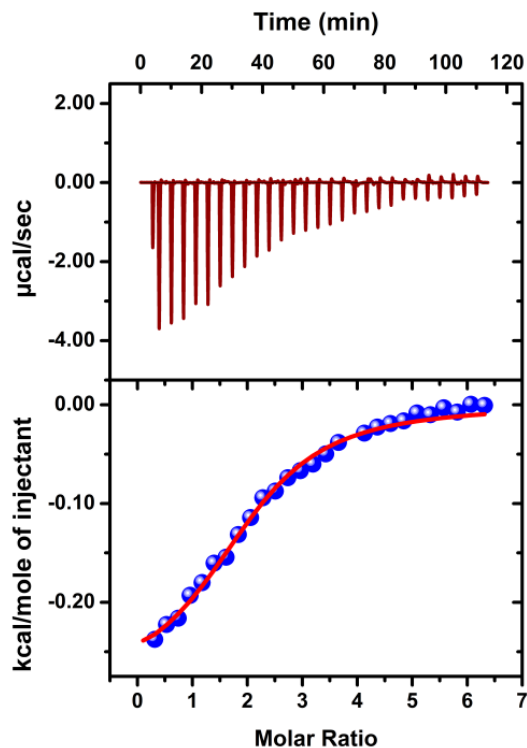


Fig. 11: Isothermal titration calorimetric (ITC) plot in CH₃CN-H₂O (1:9) at 298 K for the addition NaReO₄ (37.8 mM) to a solution of [L.6Br] (1.2 mM). The upper panel shows the experimentally determined heat pulses for each addition. The lower panel shows the individual time integrals translating as the heat evolved for each addition of aliquot and coherence to the one-site binding model.

Table S2: Association constants and thermodynamic parameters determined using isothermal titration calorimetry for [L.6Br] with NaReO₄ in 10% CH₃CN-H₂O medium at 298 K.

K_a (M ⁻¹)	2.06×10^3
ΔG^0 (kJ mol ⁻¹)	-18.9
ΔH^0 (kJ mol ⁻¹)	-1.20
$T\Delta S^0$ (kJ mol ⁻¹)	17.7

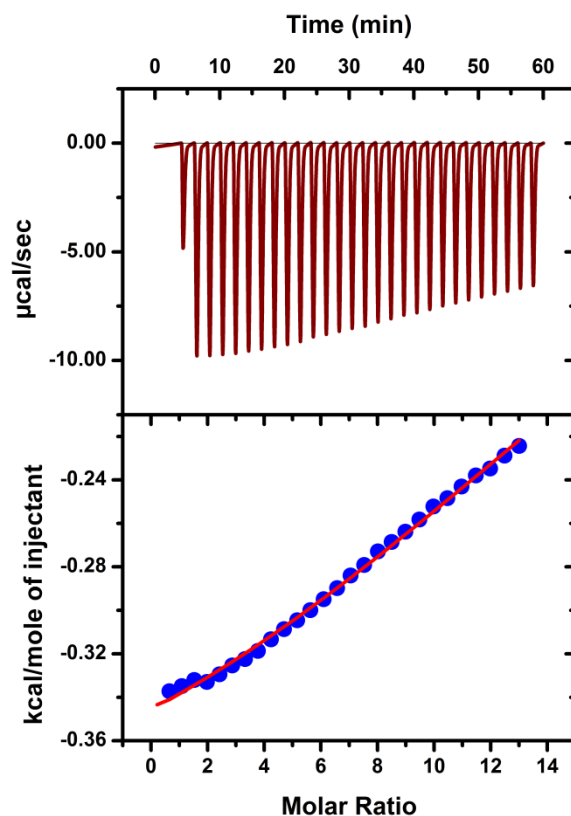


Fig. 12: Isothermal titration calorimetric (ITC) plot in CH₃CN-H₂O (1:9) at 298 K for the addition NaClO₄ (41.86 mM) to a solution of [L.6Br] (1.3 mM). The upper panel shows the experimentally determined heat pulses for each addition. The lower panel shows the individual time integrals translating as the heat evolved for each addition of aliquot and coherence to the one-site binding model.

Table S3: Association constants and thermodynamic parameters determined using isothermal titration calorimetry for [L.6Br] with NaClO₄ in 10% CH₃CN-H₂O medium at 298 K.

K_a (M ⁻¹)	145
ΔG^0 (kJ mol ⁻¹)	-12.32
ΔH^0 (kJ mol ⁻¹)	-1.79
$T\Delta S^0$ (kJ mol ⁻¹)	10.53

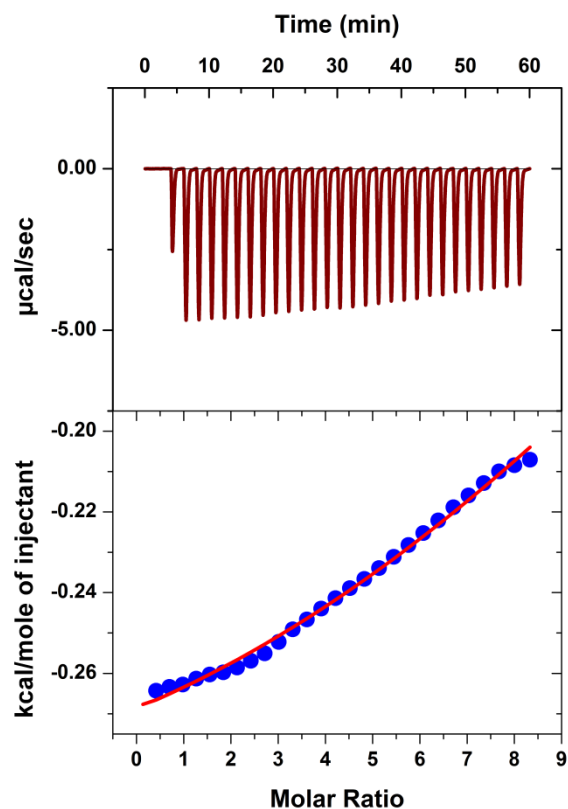


Fig. 13: Isothermal titration calorimetric (ITC) plot in $\text{CH}_3\text{CN-H}_2\text{O}$ (1:9) at 298 K for the addition NaNO_3 (35.6 mM) to a solution of [L.6Br] (1.1 mM). The upper panel shows the experimentally determined heat pulses for each addition. The lower panel shows the individual time integrals translating as the heat evolved for each addition of aliquot and coherence to the one-site binding model.

Table S4: Association constants and thermodynamic parameters determined using isothermal titration calorimetry for [L.6Br] with NaNO_3 in 10% $\text{CH}_3\text{CN-H}_2\text{O}$ medium at 298 K.

K_a (M^{-1})	317
ΔG^0 (kJ mol^{-1})	-14.18
ΔH^0 (kJ mol^{-1})	-1.28
$T\Delta S^0$ (kJ mol^{-1})	12.9

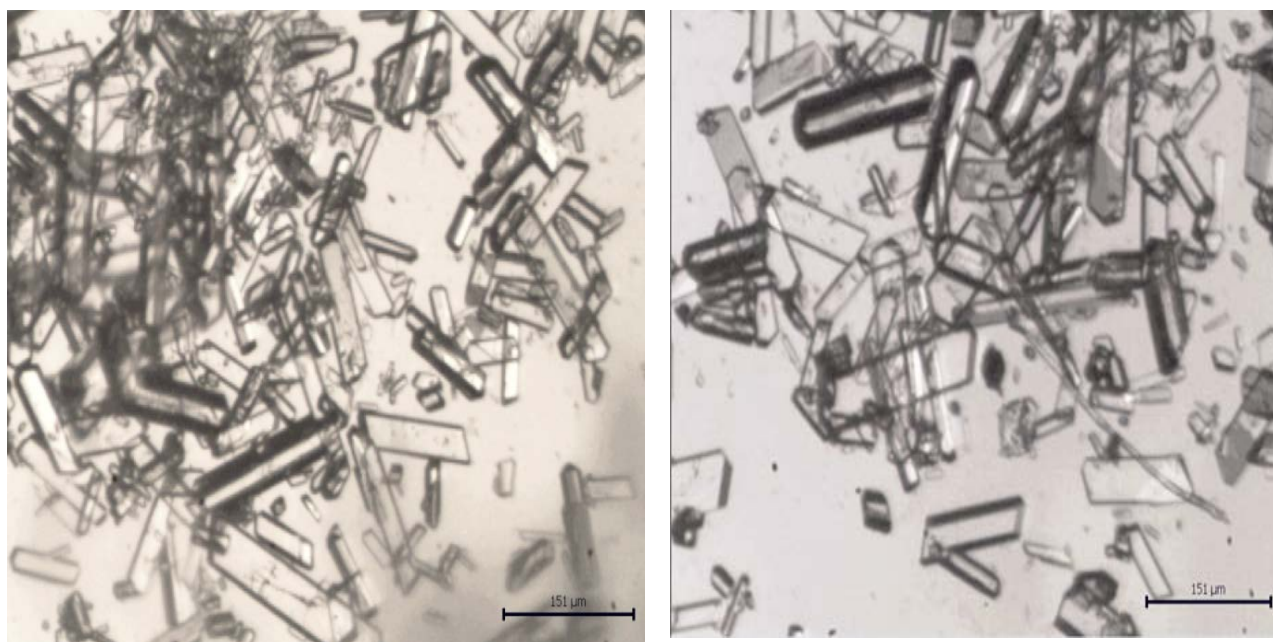


Fig. S14: Optical photograph of colorless block crystals of extracted precipitated Complex [L.6ReO₄].

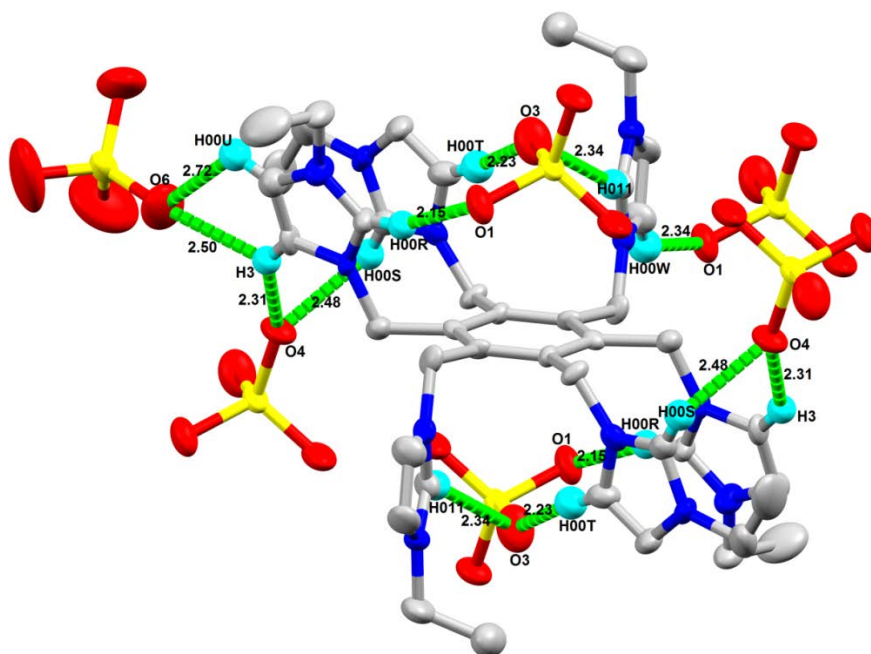


Fig. S15: Single crystal X-ray structure of [L.6ReO₄] with thermal ellipsoid drawn at the 50% probability level. Colour code; C: grey, H: cyan blue, N blue, O: red, Re: yellow. All interactive hydrogen atoms and distance(in Å unit) shown here. solvent molecules are omitted for clarity

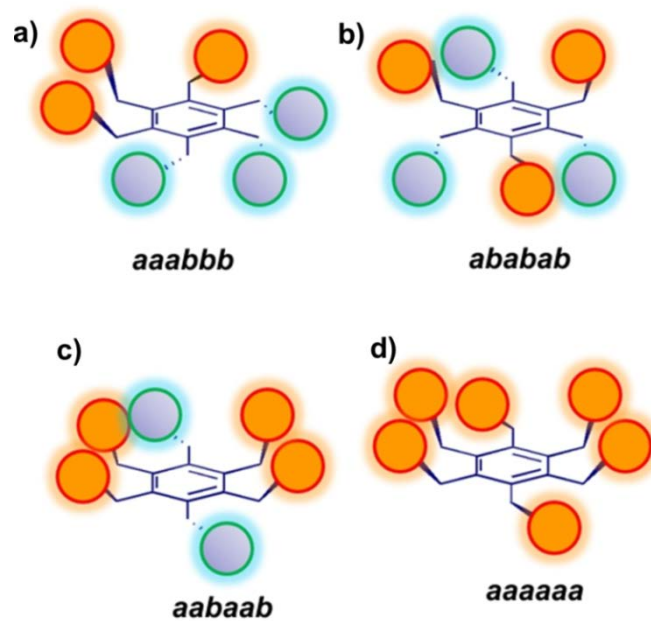


Fig. S16: Various possible conformers from of hexapodal receptors; (a) **aaabbb**, (b) **ababab**, (c) **aabaab** (d) **aaaaaa**

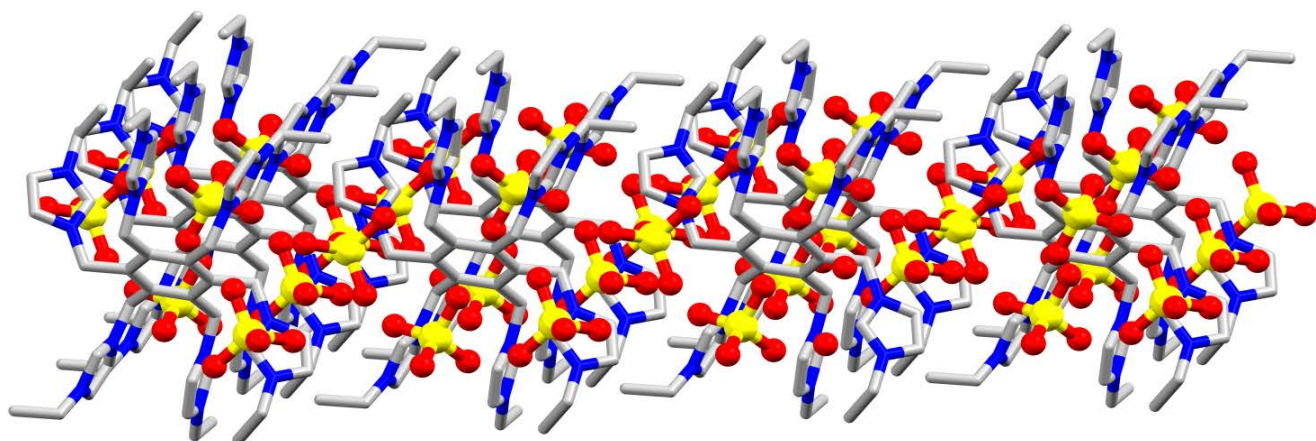


Fig. S17: Crystal packing diagram of Complex [L.6ReO₄]. Colour code; C: grey, N: blue, O: red, Re: yellow, hydrogen atoms, solvent molecules are omitted for clarity.

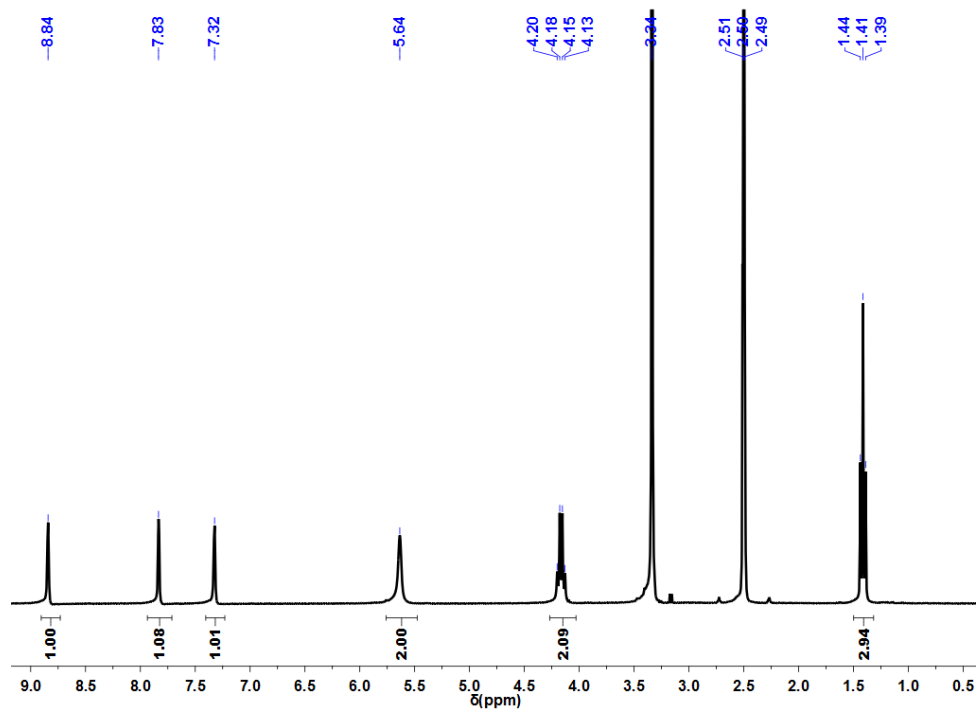


Fig. S18: ^1H -NMR spectrum of Complex $[\text{L.6ReO}_4]$ in $\text{DMSO-}d_6$ at 298 K in 300 MHz

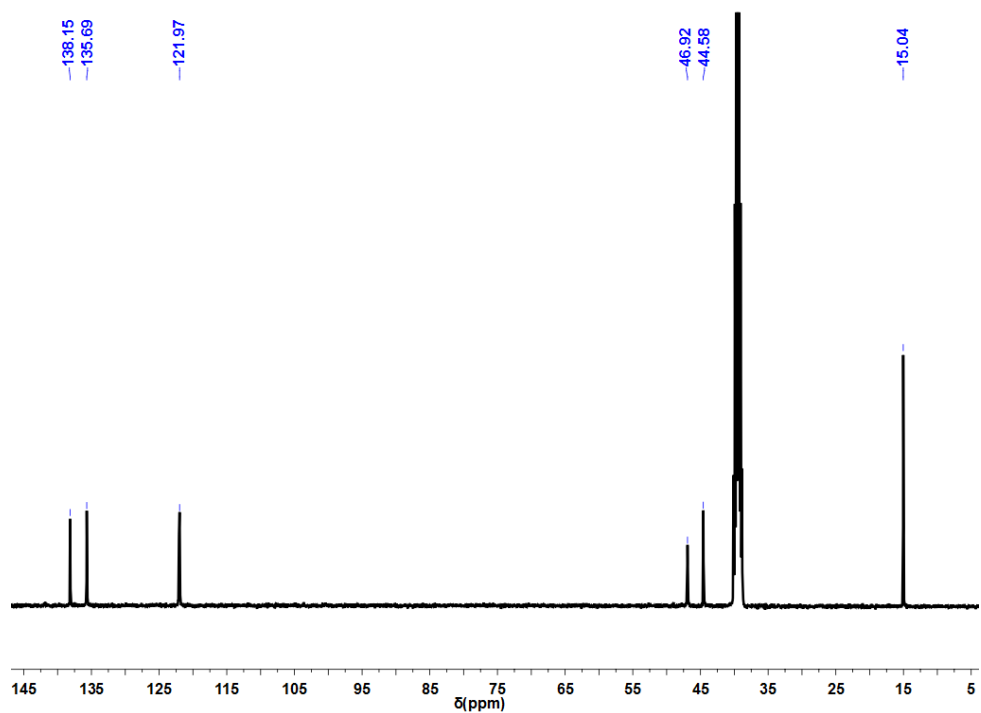


Fig. S19: ^{13}C -NMR spectrum of Complex $[\text{L.6ReO}_4]$ in $\text{DMSO-}d_6$ at 298 K in 100 MHz

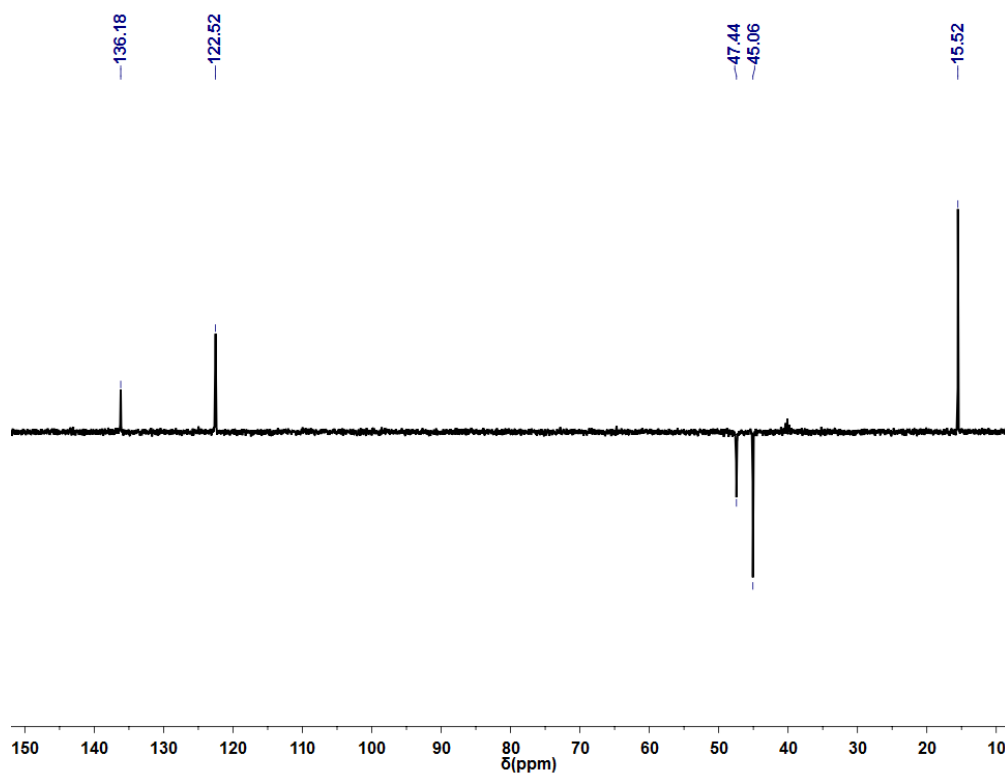


Fig. S20: ^{13}C -DEPT-135 spectrum of Complex $[\text{L.6ReO}_4]$ in $\text{DMSO-}d_6$ at 298K in 75 MHz

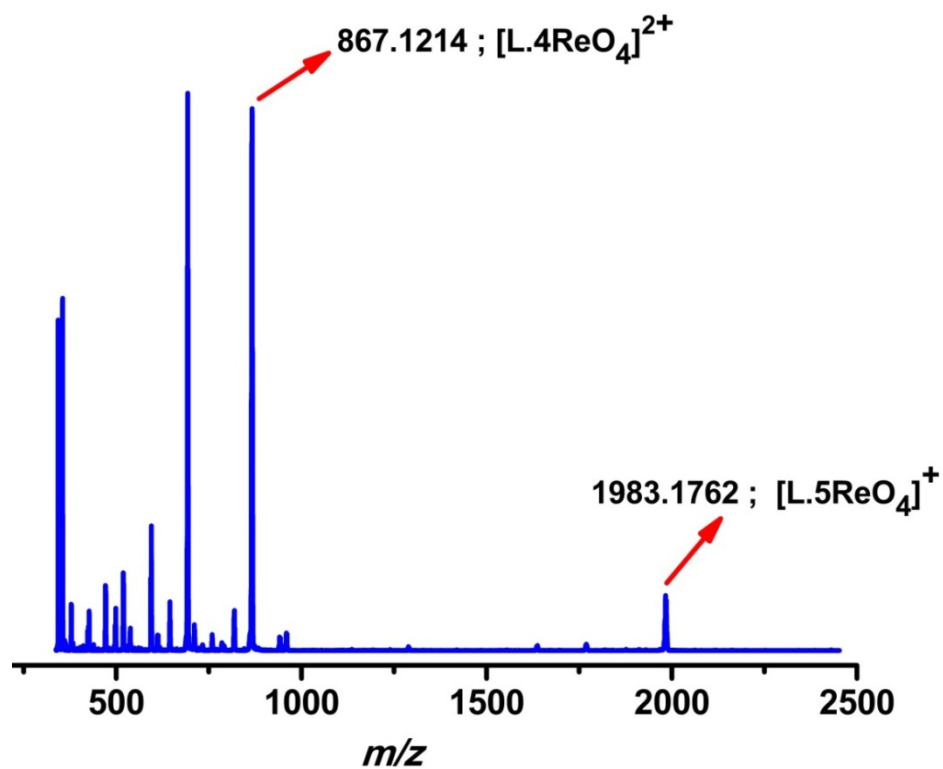


Fig. S21: ESI-MS(+ve) spectrum of Complex $[\text{L.6ReO}_4]$ at 298K.

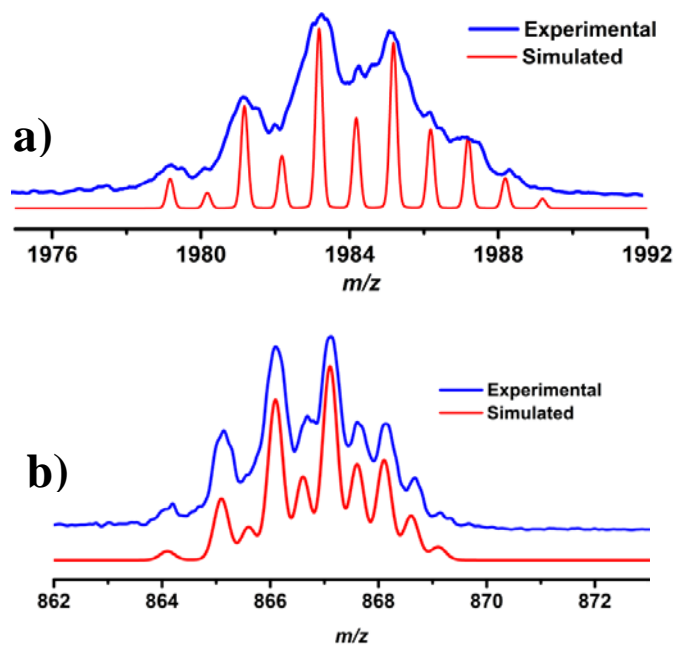


Fig. S22: Isotropic distribution of ESI-MS (+ve) spectrum of (a) $[\text{L.5ReO}_4]^+$ and (b) $[\text{L.4ReO}_4]^{2+}$ at 298K.

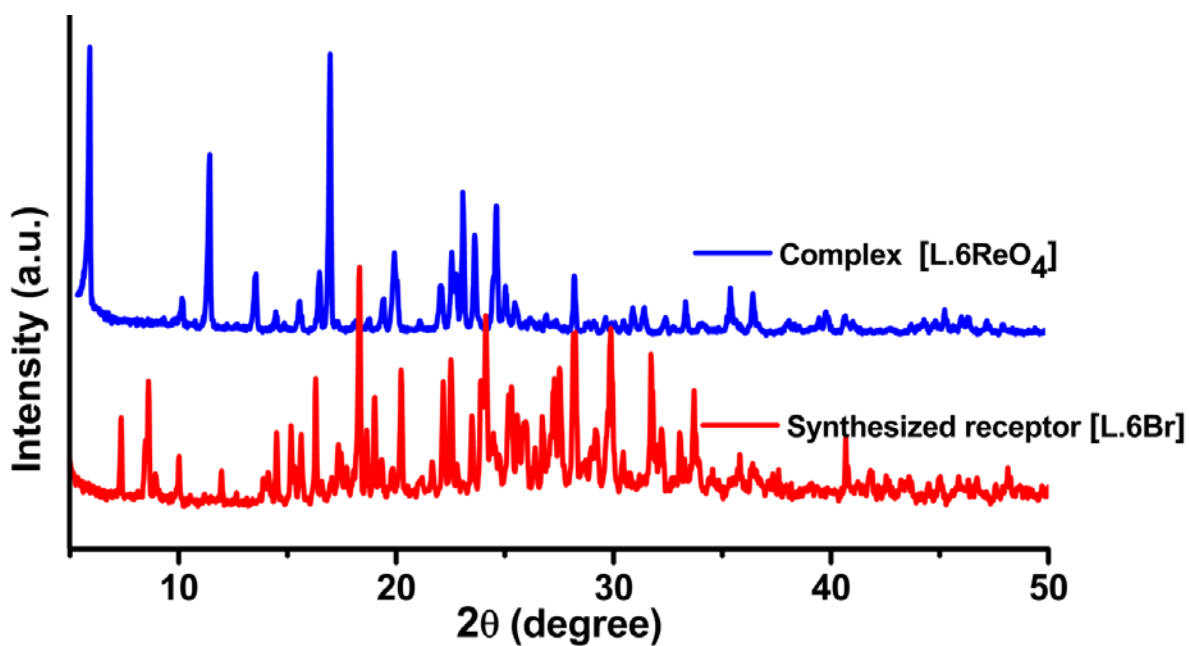


Fig. S23: A comparison of PXRD of Synthesized free receptor $[\text{L.6Br}]$ and Complex $[\text{L.6ReO}_4]$

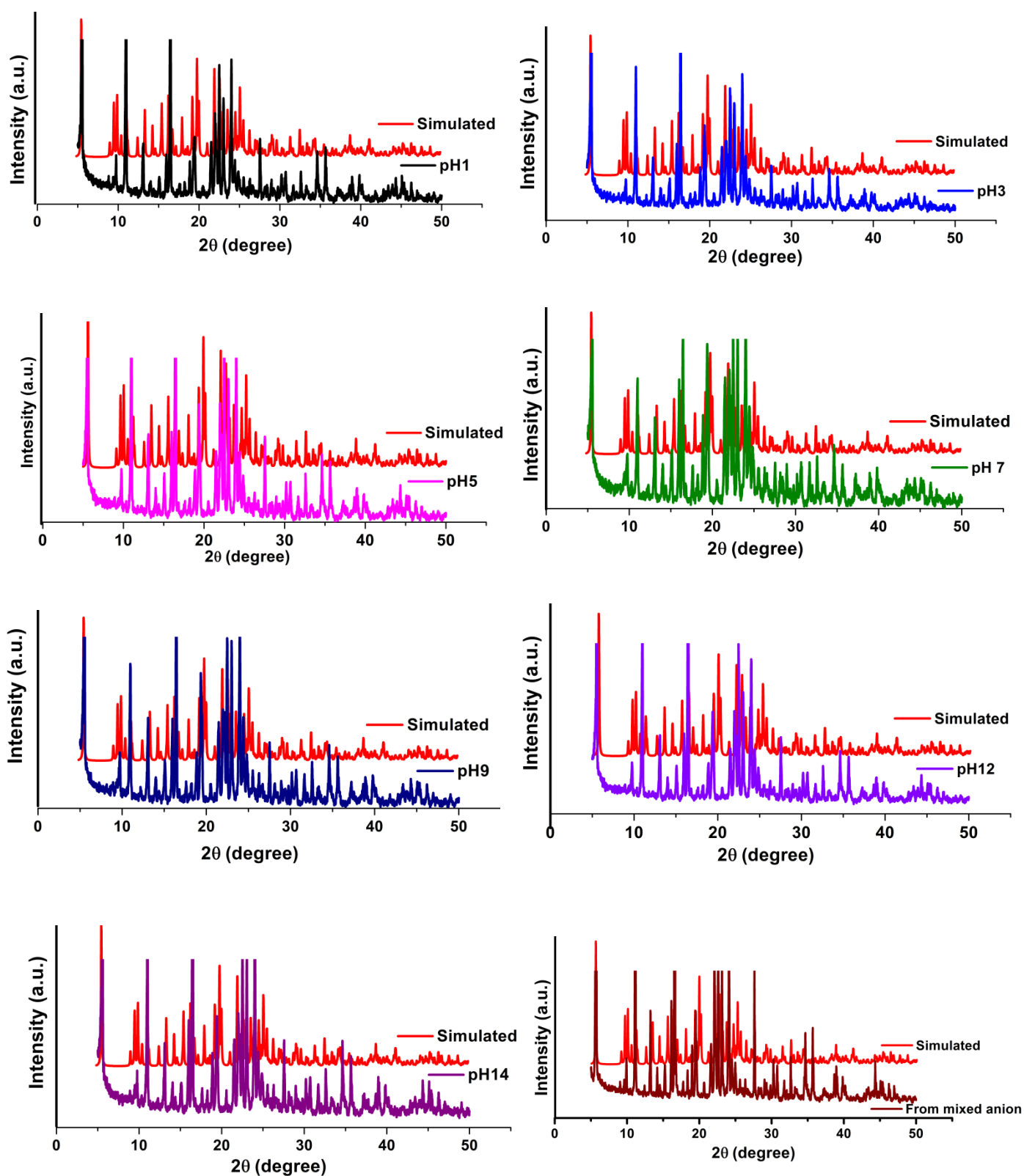


Fig. S24: Stack plot enlarge PXRD pattern of Complex [L.6ReO₄] and its comparison with simulated pattern.

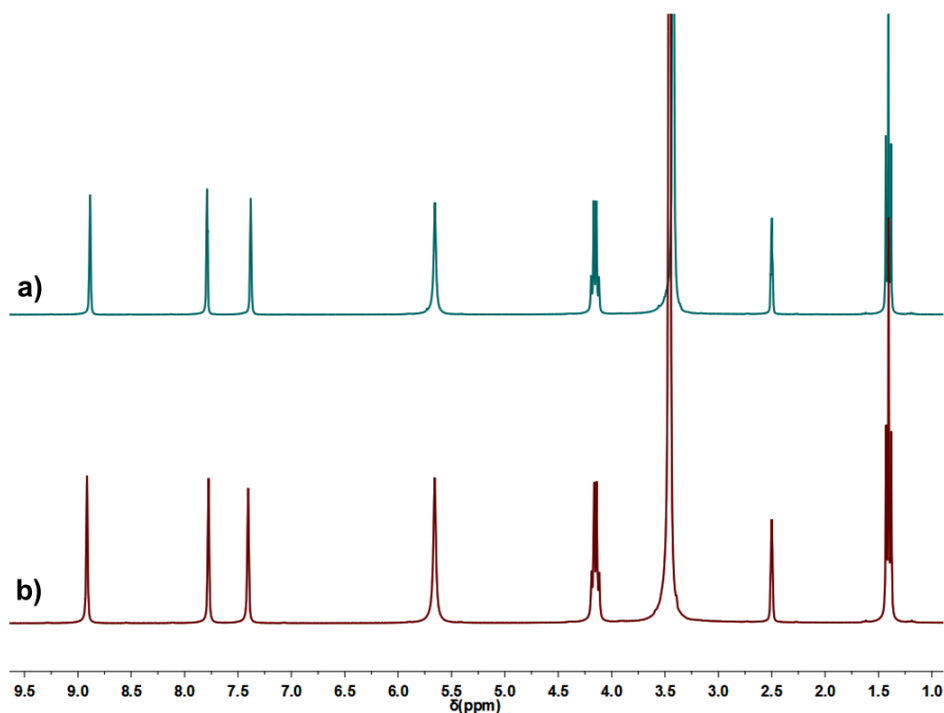


Fig. S25: Stack plot of $^1\text{H-NMR}$ spectra of (a) Extracted mass of Complex $[\text{L.6ReO}_4]$ in $\text{DMSO-}d_6$ and (b) Pure crystal of Complex $[\text{L.6ReO}_4]$ in $\text{DMSO-}d_6$ at 298K in 300 MHz

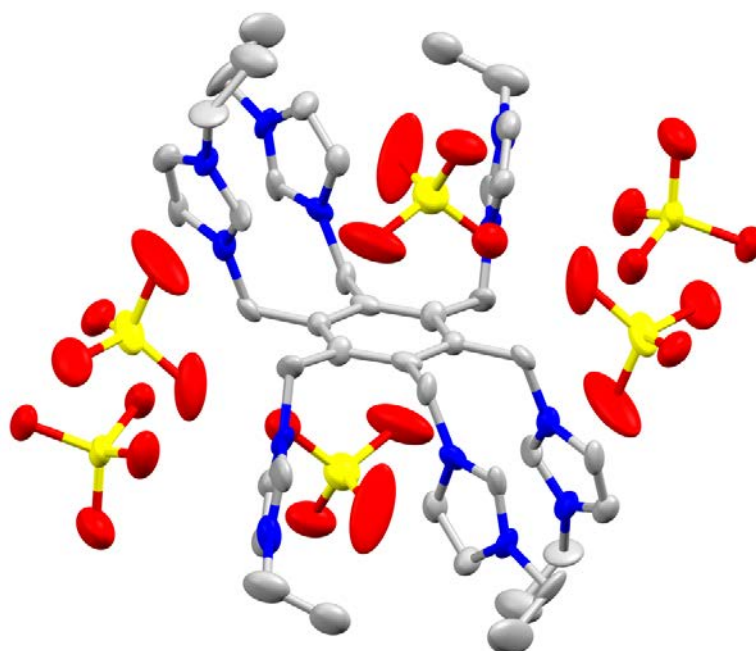


Fig. S26: Single crystal X-ray structure of of recrystallized extracted precipitated Complex $[\text{L.6ReO}_4]$ with thermal ellipsoid drawn at the 50% probability level. Colour code; C: grey, N blue, O: red, Re: yellow. Hydrogen atoms, solvent molecules are omitted for clarity

Table S5: ReO_4^- removal efficiency of [L.6Br] in presence of different concentration of ReO_4^-

Solution	Initial concentration of Re (ppm)	Final concentration of Re (ppm)	Removal Efficiency (%)
ReO_4^-	400	97.5	75.6
ReO_4^-	500	79.2	84.2
ReO_4^-	645	88.4	86.3

Table S6: ReO_4^- removal efficiency of [L.6Br] in presence of 10 equivalent amount of different anion.

Solution	Initial concentration of Re (ppm)	Final concentration of Re (ppm)	Removal Efficiency (%)
ReO_4^-	645	88.4	86.3
$\text{ReO}_4^- + \text{Cl}^-$	645	112.2	82.6
$\text{ReO}_4^- + \text{SO}_4^{2-}$	645	106.4	83.5
$\text{ReO}_4^- + \text{H}_2\text{PO}_4^-$	645	121.2	81.2
$\text{ReO}_4^- + \text{AcO}^-$	645	115.5	82.1
$\text{ReO}_4^- + \text{NO}_3^-$	645	114.1	82.3
$\text{ReO}_4^- + \text{BF}_4^-$	645	122.6	81
$\text{ReO}_4^- + \text{ClO}_4^-$	645	176	72.7
$\text{ReO}_4^- + \text{Cl}^- + \text{SO}_4^{2-} + \text{H}_2\text{PO}_4^- + \text{AcO}^- + \text{NO}_3^- + \text{BF}_4^-$	645	127.3	80.1
$\text{ReO}_4^- + \text{Cl}^- + \text{SO}_4^{2-} + \text{H}_2\text{PO}_4^- + \text{AcO}^- + \text{NO}_3^- + \text{BF}_4^- + \text{ClO}_4^-$	645	196.1	69.6

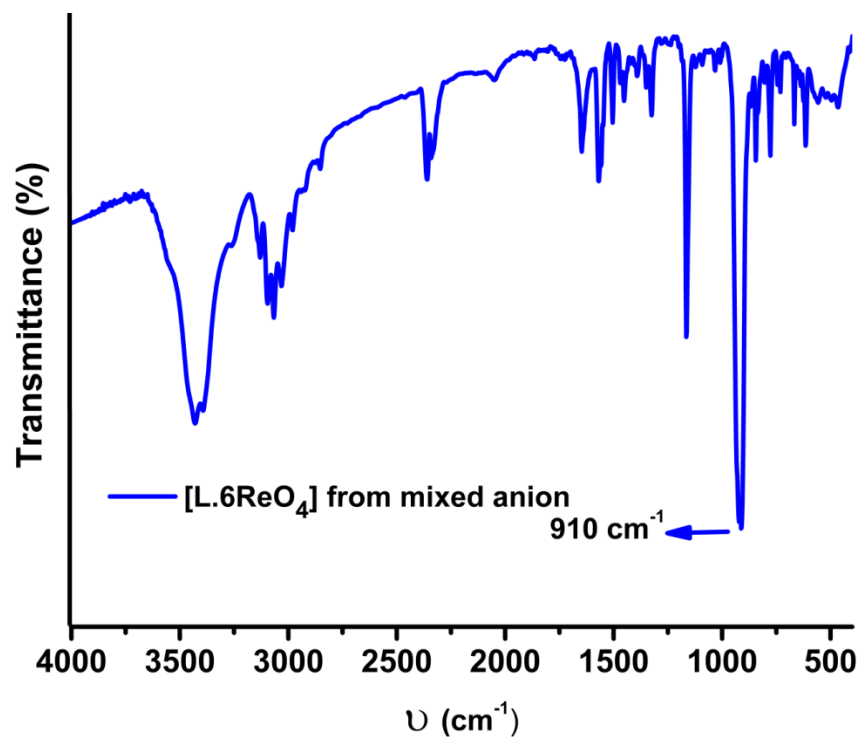


Fig. S27: FT-IR spectrum of Complex $[L.6ReO_4]$ from mixed anion (such as Cl^- , SO_4^{2-} , $H_2PO_4^-$, AcO^- , NO_3^- , BF_4^- , ClO_4^-)

Table S7: ReO_4^- removal efficiency of $[L.6Br]$ in different pH value of solution

pH	Initial concentration of Re (ppm)	Final concentration of Re (ppm)	Removal Efficiency (%)
1	630	96	84.7
3	630	91	85.5
5	630	97	84.9
7	630	100	84.1
9	630	107	83
12	630	116	81.5
14	630	121	80.7

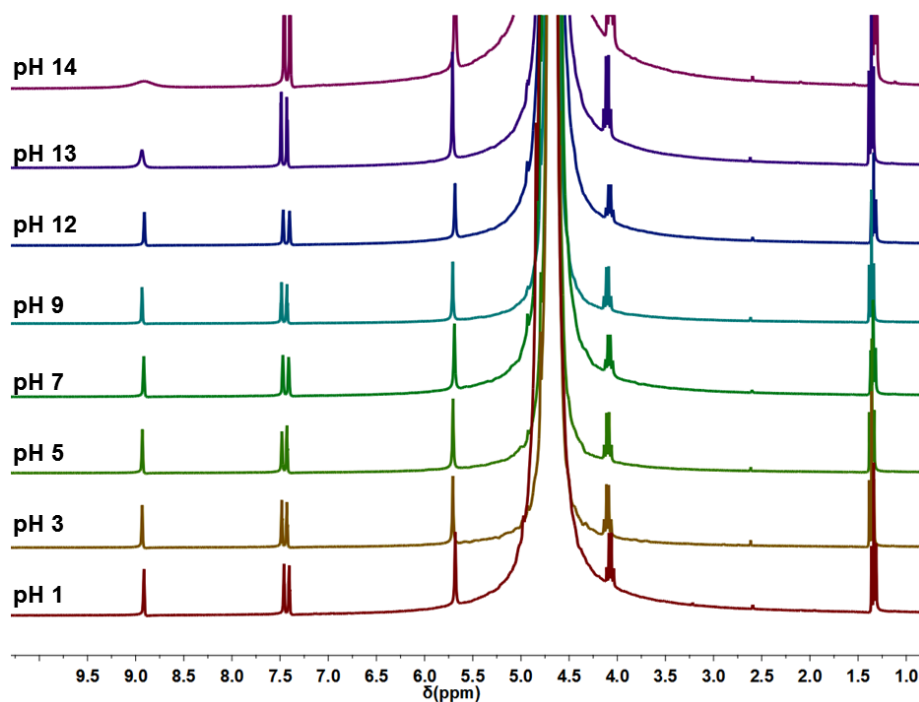


Fig. S28: ^1H -NMR spectrum of **[L.6Br]** (14.7 mM) in H_2O at different pH range in 300 MHz. (Locking was performed using a capillary tube filled with D_2O)

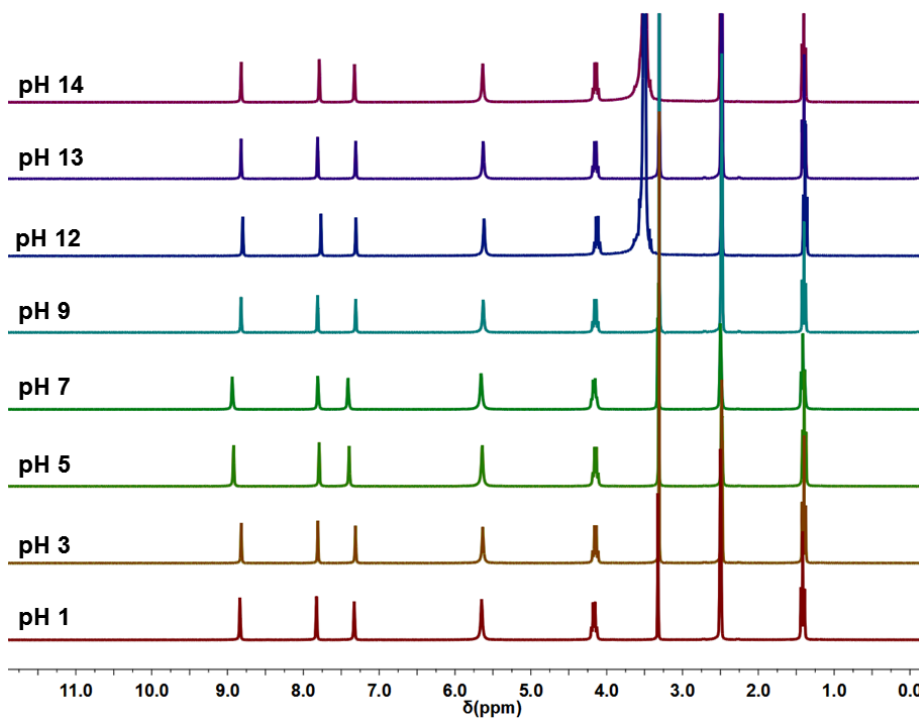


Fig. S29: ^1H -NMR spectrum of Complex **[L.6ReO₄]** in $\text{DMSO-}d_6$ 298 K in 300 MHz, after being immersed the Complex **[L.6ReO₄]** in different pH water solution for 12 hours.

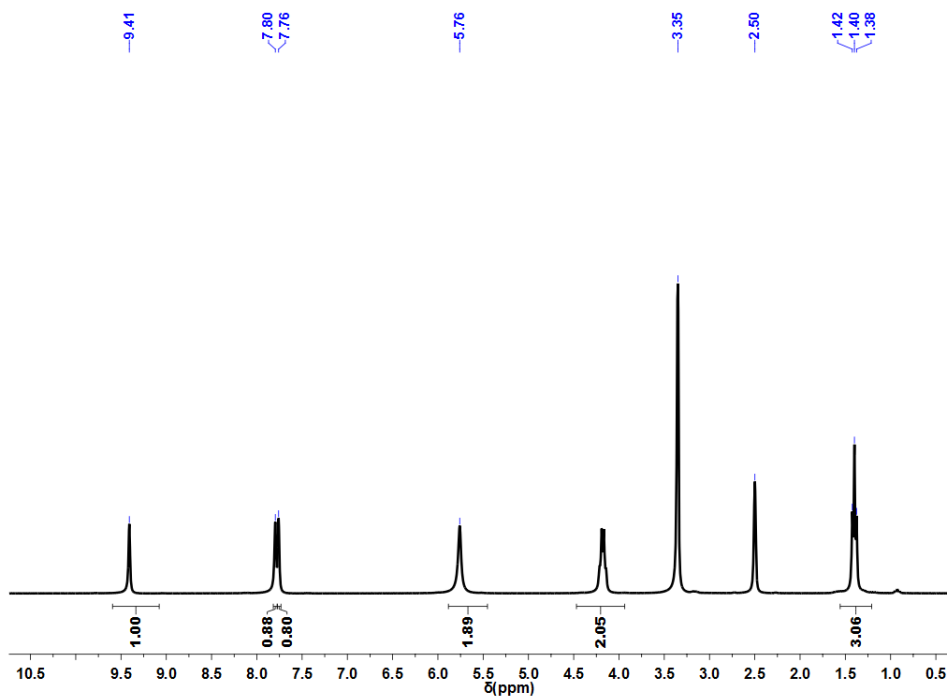


Fig. S30: ^1H -NMR spectrum of recycled **[L.6Br]** in $\text{DMSO-}d_6$ at 298 K in 300 MHz

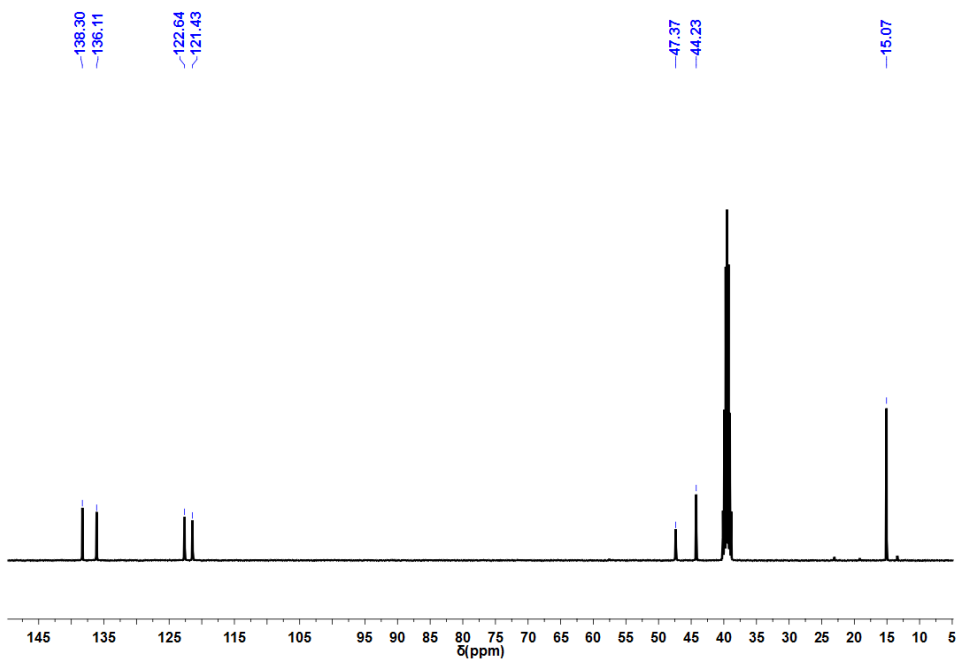


Fig. S31: ^{13}C -NMR spectrum of recycled **[L.6Br]** in $\text{DMSO-}d_6$ at 298 K in 100 MHz

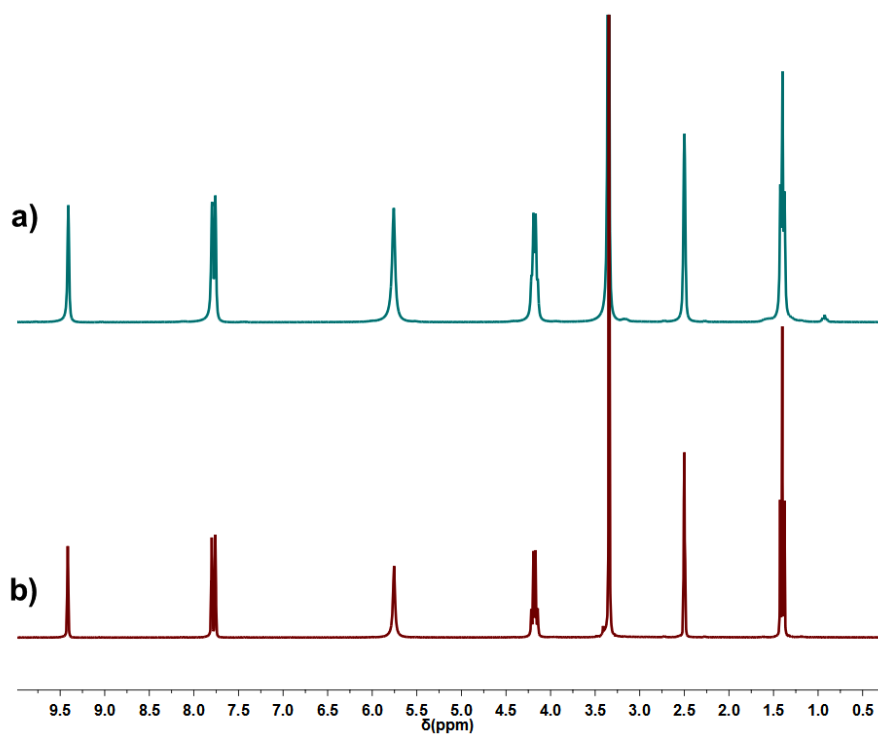


Fig. S32: Stack plot of ¹H-NMR spectra of (a) isolated mass of recycled [L.6Br] DMSO-*d*₆ and (b) pure [L.6Br] in DMSO-*d*₆ at 298K in 300 MHz

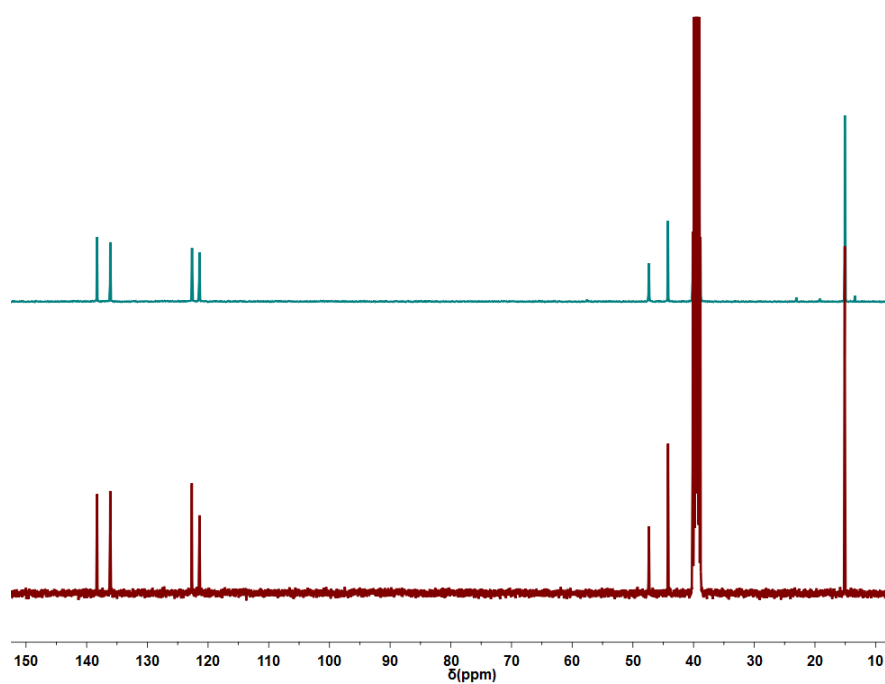


Fig. S33: Stack plot of ¹³C-NMR of (a) isolated mass of recycled [L.6Br] DMSO-*d*₆ and (b) pure [L.6Br] in DMSO-*d*₆ at 298K in 100 MHz

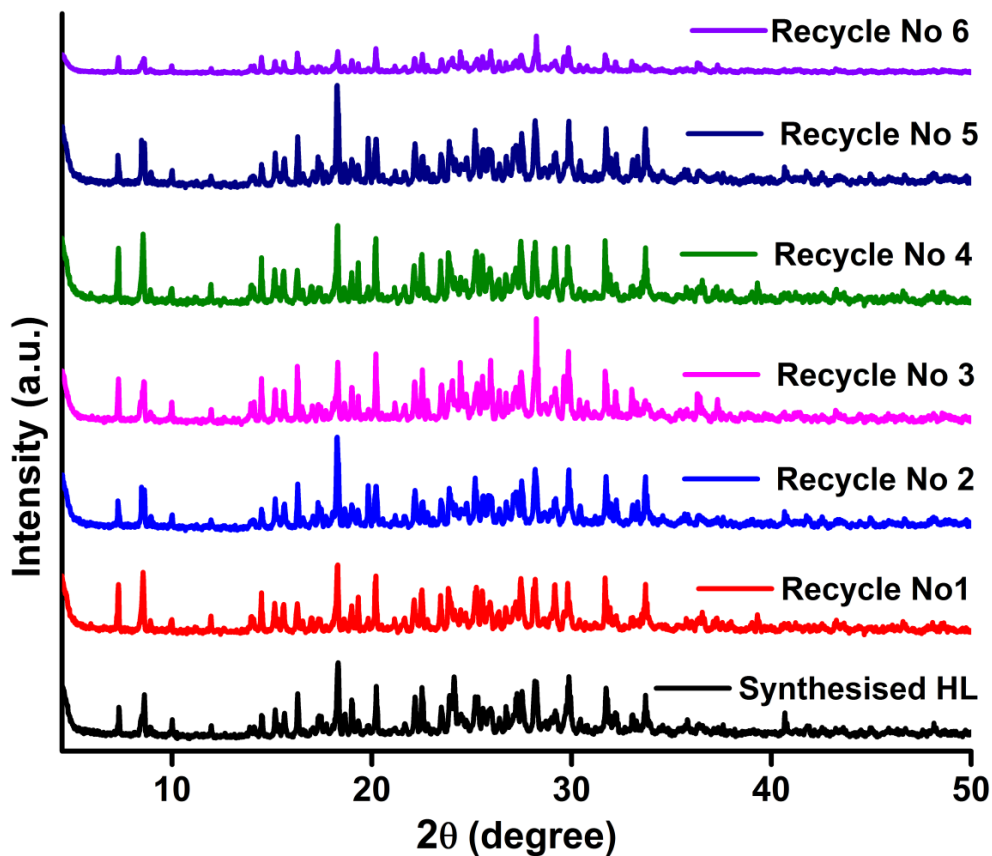


Fig. S34: PXRD stack plot of recycled receptor [L.6Br]

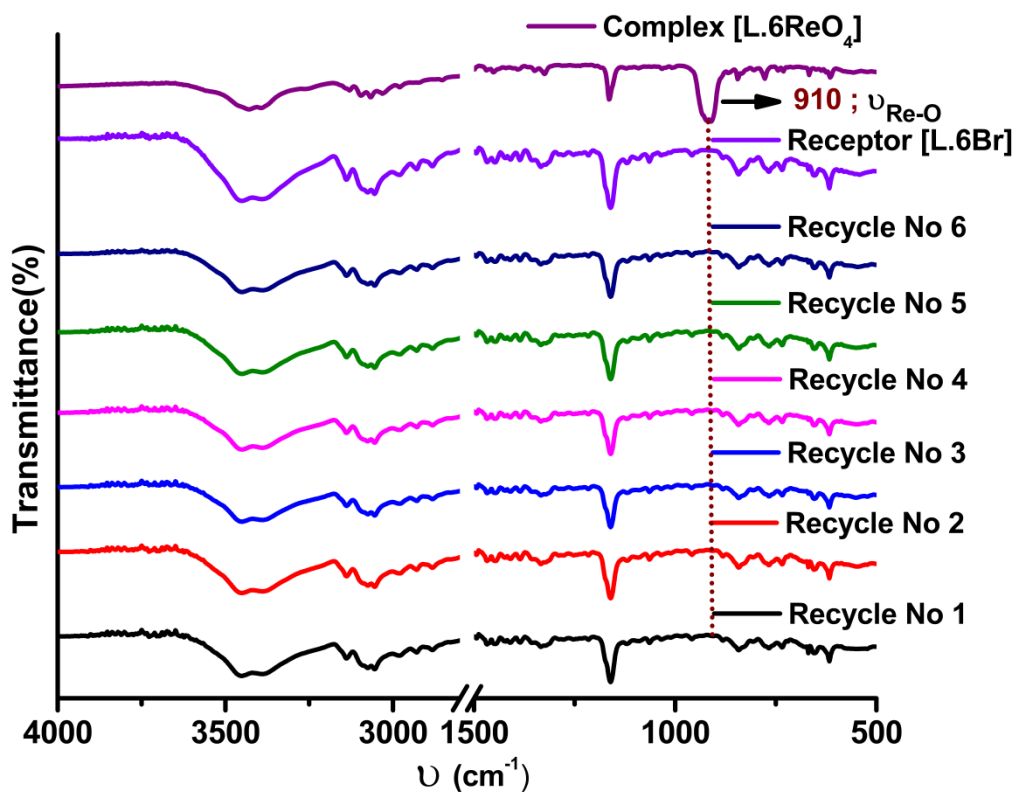


Fig. S35: IR Spectra recycled receptor [L.6Br].

Table S8: ReO_4^- removal efficiency of recycled [L.6Br].

Cycle No	Initial concentration of Re (ppm)	Final concentration of Re (ppm)	Removal Efficiency (%)
1	680.3	131.8	80.6
2	675.7	139.3	79.3
3	690.3	156.7	77.2
4	672.4	154.1	77.1
5	691.5	177.9	74.3
6	684.3	192.6	71.8

References:

- [1] SAINT and XPREP, 5.1 ed.; Sheldrick, G. M., Ed.; Siemens Industrial Automation Inc.: Madison, WI, **1995**.
- [2] SADABS, Empirical Absorption Correction Program; University of Göttingen: Göttingen, Germany, **1997**
- [3] Sheldrick, G. M. SHELXTL Reference Manual: Version 5.1; Bruker AXS: Madison, WI, **1997**.
- [4] Sheldrick, G. M. SHELXL-2014: Program for Crystal Structure Refinement; University of Göttingen: Göttingen, Germany, **2014**.
- [5] Spek, A. L. PLATON-97, University of Utrecht, Utrecht, the Netherlands, **1997**.
- [6] Mercury, version 3.7, supplied with Cambridge Structural Database, CCDC, Cambridge, U.K., **2003–2004**.